Virtual Reality Provides an Effective, Low-cost Platform for Evaluating Closed-loop Neuromyoelectric Prosthetic Hands

Journal:	Transactions on Neural Systems & Rehabilitation Engineering
Manuscript ID	Draft
Manuscript Type:	Paper
Date Submitted by the Author:	n/a
Complete List of Authors:	Kluger, David; University of Utah, Bioengineering Joyner, Janell; US Food and Drug Administration Wendelken, Suzanne; University of Utah, School of Medicine Davis, Tyler; University of Utah Department of Neurosurgery George, Jacob; University of Utah, Bioengineering Page, David Hutchinson, Douglas; University of Utah, Orthopedic Surgery Benz, Heather; US Food and Drug Administration Clark, Gregory; University of Utah, Bioengineering

Note: The following files were submitted by the author for peer review, but cannot be converted to PDF. You must view these files (e.g. movies) online.

Kluge.s3_downsampled.mp4

SCHOLARONE™ Manuscripts

Virtual Reality Provides an Effective, Low-cost Platform for Evaluating Closed-loop Neuromyoelectric Prosthetic Hands

David T. Kluger, Janell S. Joyner, Suzanne M. Wendelken, Tyler S. Davis, Jacob A. George, David M. Page, Douglas T. Hutchinson, Heather L. Benz, and Gregory A. Clark

Abstract—Although recent advances neuroprostheses offer opportunities for improved and intuitive control of advanced motorized and sensorized robotic arms, the expense and complications associated with such hardware can impede the research necessary for clinical translation. This hurdle potentially can be overcome with virtual reality environments (VREs) with embedded physics engines using virtual models of physical robotic hands. These software suites offer several advantages over physical prototypes, including high repeatability, reduced human error, elimination of many secondary sensory cues, and others. There are limited demonstrations of closedloop prostheses in a VRE, and it is unclear whether VRE performance translates to the physical world. Here we describe how two transradial amputees with neural and intramuscular implants identified objects and performed activities of daily living with closed-loop control of prostheses in a VRE. Our initial evidence further suggests that capabilities with virtual prostheses may be predictors of physical prosthesis performance, demonstrating the utility of VREs for neuroprosthetic research.

Index Terms—Electromyography, Neural Engineering, Neurofeedback, Prosthetics, Virtual Reality

I. Introduction

Prosthetic hands are becoming more advanced and more complicated to control as they more closely replicate the human form. Until recently, humans have had difficulty interfacing with these advanced prosthetic hands because of a lack of intuitive control [1]. One way that control can be improved is through the use of neuromuscular implants, which record neuromuscular activity with a high signal-to-noise ratio and high channel count. Such implants offer improved decoding of intended motor movement by increasing signal-to-noise

This manuscript was submitted for review on August 29th, 2018. This work was jointly sponsored by DARPA MTO SPAWAR Pacific Grant/Contract No. N66001-15-C-4017 and NSF BCS #1533649.

- D. T. Kluger, J. A. George, and G. A. Clark are with the University of Utah's Department of Bioengineering, Salt Lake City, UT 84112 USA (emails: david.kluger@utah.edu, jake.george@utah.edu, greg.clark@utah.edu).
- J. S. Joyner is an Oak Ridge Institute for Science and Education (ORISE) Research Fellow at the US Food and Drug Administration, Silver Spring, MD, 20993 (email: Janell.joyner@fda.hhs.gov).
- H. L. Benz is with the US Food and Drug Administration, Silver Spring, MD, 20993 (e-mail: heather.benz@fda.hhs.gov).

ratios of myoelectric recordings and are capable of providing signals for many degrees of freedom (DOFs) to be controlled [2]–[4]. Furthermore, these interfaces can be used to stimulate residual nerve fibers, creating a bidirectional, closed-loop system between a sensorized prosthetic device and an amputee that improves the functionality of the prosthesis [5]–[8].

The potential benefits of these new closed-loop neuromuscular prosthetic systems need to be demonstrated, but doing so with a physical limb introduces some challenges, including, but not limited to, a high upfront cost for a prosthesis, prosthesis maintenance, and socket fitting [9], [10]. Researchers can still test these systems without a physical prosthesis and remove all of the aforementioned challenges by using a virtual prosthetic hand (VPH) in a virtual reality environment (VRE) with an embedded physics engine instead of a physical prosthesis in the physical world [11]. In addition, VREs offer potential advantages. Because the VPH is not physically tethered to an amputee's residual limb, secondary cues from skin-socket interactions and sounds are non-existent. Replicating trials is also highly repeatable both within a laboratory and among different laboratories, because of the ability to reload experimental scenarios instantly in exactly the same way as they were previously rendered. Previous work has shown that VREs can be useful for testing motor capabilities alone [12]-[14], but did not perform closed-loop tests, presumably due to an inability to provide sensory feedback.

Beyond allowing the investigation of closed-loop prosthetic arm control capabilities, such as object identification tasks, VREs also offer an excellent way to observe how complex behaviors change with the presence or absence of feedback applied through peripheral nerve stimulation. VREs provide a low-level experimental playback capability that allows for every contact interaction to be digitally logged. For complex freeform experiments, this playback capability allows for

- S. M. Wendelken was with the University of Utah's Department of Bioengineering, but is now with the University of Utah School of Medicine, Salt Lake City, UT 84132 USA (e-mail: Suzanne.wendelken@hsc.utah.edu).
- T. S. Davis is with the University of Utah's Department of Neurosurgery, Salt Lake City, UT 84132, and Ripple LLC, Salt Lake City, UT 84106 (e-mail: tyler.davis@hsc.utah.edu).
- D. M. Page was with the University of Utah's Department of Bioengineering, but now works with Halyard Health Global, Alpharetta, GA, 30004 (e-mail: dmpage88@gmail.com).
- D. T. Hutchinson is with the University of Utah Department of Orthopaedics, Salt Lake City, UT 84108 (e-mail: douglas.hutchinson@hsc.utah.edu).

nuanced closed-loop control behavior to be analyzed beyond the simple outcome metrics of time-to-completion or difficult-to-blind experimenter observations. Using VREs allows for extremely tight time-synced analyses between motor control and sensory output, which is not feasible to perform with simple experimenter observations. Furthermore, mechanical constraints of sensor activation and overcoming joint friction amount to lag in physical systems that can confound analyses of subtle sensorimotor interactions, which virtual motors and sensors can completely bypass. These analytical advantages promote the use of VREs for investigating the changes in prosthetic hand control caused by sensory feedback.

We herein describe experiments conducted with two human transradial amputees performing tasks with bi-directional closed-loop control of a VPH. The results from these experiments demonstrate that VPHs within VREs can serve as a useful tool for researchers attempting to validate and quantify their control systems for high-DOF sensorized prosthetic hands. These experiments demonstrate that contact interactions between a VPH and virtual objects can be used to drive intraeural microstimulation useful for better understanding a virtual environment, and highlight the impact of bidirectional close-loop control on both motor behavior and sensory processing. Furthermore, the stimulation that was provided in response to these virtual interactions can be translated to a physical-world system in order to provide an amputee with the same benefits stimulation provided in a virtual world.

II. MATERIALS AND METHODS

A. Patients

Two transradial amputee volunteers provided informed consent under guidance by a University of Utah IRB and Department of the Navy Human Research Protection Program in this study as a part of the Defense Advanced Research Projects Agency's HAPTIX program. The first volunteer (HS1) was a bilateral upper-extremity amputee, whose amputation occurred 24 years prior to the investigation. The second volunteer (HS2) was a dual left transradial and transtibial amputee whose amputation occurred 12 years prior. Both volunteers had their left arms implanted with neuromuscular implants with the same surgical procedure.

B. Implants and Surgery

The volunteers were put under general anesthesia. Two wired Utah Slanted Electrode Arrays (USEAs, Blackrock Microsystems, Salt Lake City, UT) consisting of 100 penetrating microelectrodes of varying length were implanted, 1 array per nerve, into the median and ulnar nerves of the left upper arm [15]. A wired intramuscular electromyography recording implant (iEMG, Ripple LLC, Salt Lake City, UT) consisting of 8 leads with 4 electrodes each plus 1 reference lead was implanted into residual muscle of the left forearm. Wires from the implants travelled subcutaneously from the implant site to individual transcutaneous sites on the posterior upper arm. iEMG leads travelled along the back of the elbow to reach the transcutaneous site. External Gator (Ripple LLC) connectors were wire-bonded to the extracutaneous portions of the wires, which served as the mounting point for Grapevine (Ripple LLC) stimulating and recording hardware. Volunteers were given at least 1 week to recover from surgery before experiments began.

C. VRE

We used the Multi-Joint dynamics with Contact VRE (MuJoCo, Roboti LLC, Redmond, WA) provided through the DARPA HAPTIX program for closed-loop experiments [11]. MuJoCo was chosen for this application because this VRE has a built-in physics engine that calculates contact interactions between objects. Simulations were built using .XML script, and real-time inputs to and outputs from the VRE were managed through a MATLAB (Mathworks®, Natick, MA) application program interface (API). We recorded calculated contact forces on individual hand segments in real time. Similarly, we controlled individual segments of the hand independently, which allowed for individual control of the digits and wrist through the API. MuJoCo's data logging of the VPH's movements and contact with the VPH's sensors occurred at 1 kHz.

Volunteers used 1 of 2 VPH models for these experiments. HS1 used a virtual Modular Prosthetic Limb (vMPL, Johns Hopkins Applied Physics Lab, Laurel, MD). This VPH had 19 contact sensors spanning the fingers, palm, and back of the hand: palmar sensors on every phalangeal segment of every finger, 2 on the palm, 1 on the lateral edge of the hand, and 1 on the back of the palm. The vMPL had 13 motors: 1 for flex/extend on each finger, 1 ab/adduction on the index and on the little fingers, 1 each on the 4 joints of the thumb, and 3 for the wrist individually controlling flex/extend, supinate/pronate, and ulnar/radial deviation. Each motor had position feedback, giving a total of 32 sensors.

HS2 used a virtual LUKETM Arm (vLA, DEKA Research Corporation, Manchester, NH). This hand had 11 contact sensors: 1 on the tip of each digit, lateral sensors on the distal phalangeal segments of the thumb and index, 2 on the palm, 1 on the lateral edge of the palm, and 1 on the back of the palm. The vLA had 6 motors: 1 for index flex/extend, 1 for combined middle/ring/little (MRL) flex/extend, 2 for the thumb controlling flex/extend (thumb yaw) and ab/adduction (thumb pitch), and 2 on the wrist controlling supinate/pronate and flex/extend. Each motor had position feedback, giving a total of 17 sensors. (More recent physical and virtual LUKETM Arm models, not used in the present studies, have added 2 contact sensors to the lateral and posterior sides of the thumb.)

D. Hand Calibration

Decoding of motor movements has been previously described [6], [16]. In addition to using firing rate of neural discharges recorded by USEA electrodes as potential features for a modified Kalman-filter-based decode, we used the mean absolute value of the filtered recordings from all possible 528 single-ended and differential pairs of the 32-lead iEMG [17]. Once the modified Kalman-filter-based decode was trained, decoded movements were tied to motors of 1 of the 2 VPHs, which allowed for real-time individual and proportional control of the motors of the hand. Modifications to a standard Kalman filter included use of thresholds and non-unity gains, which were adjusted by an experimenter to allow for full range of motion within a DOF and to minimize crosstalk between DOFs [17], [18].

Motors could be moved in a "velocity" or "position" mode, and the mode of each DOF was independently toggled depending on the task. Velocity control is employed by conventional myoelectric prostheses; the joint angle of a given motor stays constant until a flex or extend signal is detected, at which time the motor moves. Position mode has a rest joint angle, and the DOF will return to this rest position when no intended movements are detected. The distance the joint moves from rest is correlated to the intensity of the decoded signal.

When enabled, movements of the entire VPH through virtual space were mediated by movements of a volunteer's residual forearm. An OptiTrack V120:Trio (Natural Point, Inc., Corvallis, OR) infrared camera tracked retroreflective markers placed on the residual forearm and on the computer monitor that rendered the virtual simulations. Motive software (Natural Point, Inc.) computed the movements of the forearm relative to the monitor, and moved the VPH through virtual space accordingly.

Sensory calibration necessitated stimulation mapping of each of the 192 combined active channels of both implanted USEAs [6], [7], [17], [19]. The orientation and numbering of the array's electrodes can be seen in supplementary Fig. S1. The modality of the sensations varied, but the modalities included cutaneous and proprioceptive sensations across the volunteers' phantom hands. Electrodes evoking cutaneous sensations were mapped to contact sensors of the VPH, whereas electrodes evoking proprioceptive sensations were mapped to the joint-angle sensors of the VPH. During bidirectional, closed-loop control of the VPH, the stimulating and recording software operated at a 30-ms loop cycle.

After we had identified individual or groups of electrodes capable of evoking sensations congruent to the prosthesis sensors, we explored the sensation intensity range on those electrodes with either amplitude and/or frequency modulation. Stimulation was delivered in continuous 500-ms bursts separated by 500 ms of no stimulation. Individual pulses within the bursts were cathodic-first, charge-balanced square waveforms with 200-µs single-phase durations separated by a 100-µs interphase interval. We asked the patient to rate the perceived intensity on a 0–10 verbal scale while we adjusted the current and/or frequency of the pulses within the bursts. We set lower limits of amplitudes and frequencies for which the volunteer could barely feel the stimulation, or reply with an intensity greater than zero and less than or equal to 1, so that any touch between the VPH's contact sensor would result in a noticeable sensation. We then manually increased the amplitude and/or frequency on the same electrode(s) to identify stimulation upper limits, which were bound by safety and software limits of 500 Hz and 100 µA. Upper limits were chosen to coincide with the maximum bearable intensity of the evoked sensation while being below the safety limits. The perceived intensities of the maximized stimulation parameters were usually in the range of 2-5 in the self-reported scale. These minimum and maximum amplitudes and frequencies were set to define the range of intensities our volunteers could possibly experience with VPH interactions.

We often introduced temporal variability to the USEA stimuli, i.e. jitter, in order to make the artificially-produced sensations more realistic, a phenomenon that has been reported

in the literature [5]. We created jitter by systematically changing the pulse train frequency during each 30-ms loop cycle. Jitter was encoded by adding Gaussian noise to the stimulation frequency with a standard deviation of half the scaled frequency, which was calculated by linearly scaling the sensor output to the minimum and maximum frequencies found from sensory calibration.

If stimulation could not be detected below our upper limit, we sometimes added another electrode that generated a similar sensation and repeated the calibration procedure. In some cases, we could not generate sensations of varying intensity due to our frequency and amplitude limits and a lack of available percepts that had been revealed from stimulation-mapping sessions. In these cases, we would abandon attempting to encode the anatomically-matched VPH sensor. All of the sensory encode parameters for both volunteers can be seen in supplementary Table S2.

E. Open-loop Sensory Task

We tested HS2's ability to discriminate among the location and intensity of stimulation driven by the VPH's sensors on 2 occasions. The volunteer was presented with stimuli that varied by sensor location, modality (i.e., contact or joint movement), and intensity (i.e., contact force or amount of movement).

For the first experiment, HS2 discriminated between cutaneous sensations with 3 discrete intensities (i.e., discrete stimulation frequencies) and 4 discrete locations (i.e., discrete USEA electrodes) for a total of 12 possible options. The four discrete locations were independently tied to the lateral palm, distal index, distal thumb and thumb joint position sensors (sensory substitution) of the VPH. The second experiment used only the aforementioned contact sensors without the thumb joint position sensor at 4 intensities using amplitude modulation on 4 USEA electrodes. HS2 had the opportunity to feel the stimulus up to 5 times before he had to guess which stimulus had been presented to him. Each stimulus lasted for 1 second. Jitter was used during both experiments.

We performed binomial tests of the volunteer's responses to assess whether he could identify the stimuli. We rejected the null hypothesis of an inability to identify a stimulus property at a familywise error rate of $\alpha = 0.05$ using Holm-Šidák-Bonferonni corrections for multiple comparisons.

F. Closed-loop Tasks

1) Size and Compliance Identification: Both HS1 and HS2 performed virtual size-identification tasks with motion capture disabled. HS1's size-identification task involved randomly positioning the vMPL beneath empty space, a small 3.5-cm diameter cylinder, or a large 8-cm diameter cylinder. All 4 fingers moved in tandem using the decoded signal from a single DOF. The volunteer had unlimited time to explore the virtual space above the vMPL and attempt to identify what was positioned over the hand. After the volunteer guessed the object's size, feedback was given towards his response and the next object was presented immediately. Proportional proprioceptive sensory feedback was provided by frequency modulation of 2 electrodes and binary cutaneous sensory feedback (i.e., on or off) was delivered through 3 electrodes.

Transactions on Neural Systems and Rehabilitation Engineering

HS2's object-identification task required identifying objects of varying size and compliance with position control of the vLA. The volunteer had to identify both the size and compliance of a randomly selected object placed over the vLA's palm by squeezing the virtual objects. HS2 had 30 s to explore the object and attempt to identify its size and compliance while blindfolded. After the 30-s exploration duration expired, a mandatory inter-trial interval of 45 s was used to minimize sensory adaptation [20]. For the first test, the volunteer discriminated among 4 unique objects with large or small size (diameter of 4 cm or 8 cm) and a soft or hard compliance (damping ratio and spring constant of 222 and 400 or 1010 and 2000, respectively). We provided the volunteer with position control of the index and MRL DOFs, which were coupled together. The experiment used frequency- and amplitude-modulated intensity encoding through 2 electrodes with jitter.

The second test was made more difficult by adding mediumsized and medium-compliance objects, yielding a 3x3 confusion matrix. All of the objects presented to the volunteer can be seen in Fig. 1. The medium objects were 6 cm in diameter. Their damping ratios and spring constants were 421 and 800, respectively. Again, the index and MRL DOFs were coupled together and driven by position control. The experiment consisted of 36 trials with the same trial timing as the 2x2 experiment. We delivered frequency- and amplitudemodulated intensity encoding with 1 electrode, with jitter on the first and no jitter on the second.

To compare virtual and physical closed-loop task performance, HS2 performed a similar 2x2 size/compliance identification task with closed-loop position-control of a 3Dprinted Ada Hand (Open Bionics, Bristol, UK) with forcesensitive resistors embedded in the 3D-printed material serving as contact sensors. The hard objects were a golf ball and a lacrosse ball, and the soft objects were similarly-sized foam balls. The volunteer was blindfolded and had control of the Ada Hand's middle finger. Frequency- and amplitude-modulated intensity encoding was used on 1 electrode with no jitter.

2) Texture Identification: A pilot study of HS1 stroking a virtual door under closed-loop control of the vMPL indicated he could feel the door. Because of his reactions to this pilot test, we developed a regimented texture-identification task for HS2.

HS2 performed a texture discrimination task with motion capture enabled on the vLA. Either a smooth wall or a wall with 4-cm corrugations was randomly placed in the virtual environment while the volunteer was blindfolded and had sensory-only control or closed-loop control of the VPH (Fig. 2). The volunteer stroked the wall using motion capture and had to guess which wall was present for 30 s with a 90-s break to minimize sensory adaptation. Control of the motors was disabled for the first 12 iterations of this test, whereas the second 12 trials allowed the volunteer to independently control the index motor, and coupled and middle, ring, and little finger motors using position control. We delivered frequency- and amplitude-modulated intensity encoding on 1 electrode with jitter.

For the aforementioned size, compliance, and texture discrimination tasks, we performed binomial tests of the volunteer's responses to assess whether he could identify the objects' properties. We rejected the null hypothesis of an

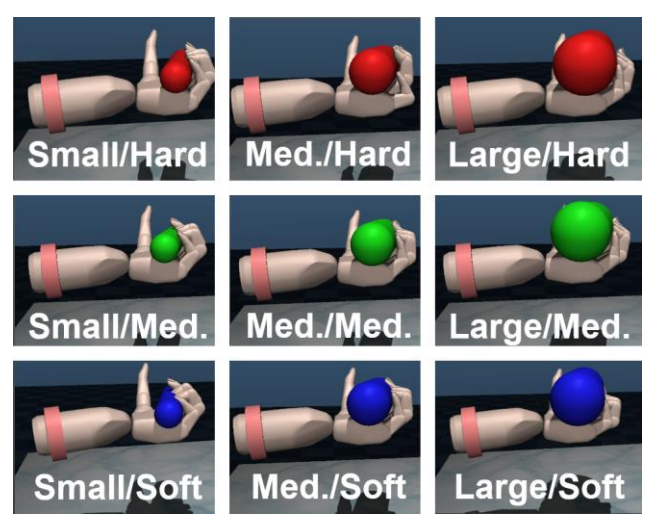


Fig. 1. All objects presented to HS2 for the virtual size/compliance identification tasks. The 2x2 task used the 4 objects in the corners whereas all objects were used for the 3x3 task.

inability to identify an object property at a familywise error rate of $\alpha = 0.05$ using the Holm-Sidák-Bonferonni method of multiple comparisons.

3) Activity of Daily Living (ADL) tasks: Both HS1 and HS2 performed virtual tasks that simulated literature-validated ADL assessment procedures. HS1 performed a subset of virtual Action Research Arm Test (ARAT) tasks without a time limit [21]. We added concave features to the faces of the 2-cm and 4-cm cubes to improve the virtual hand's grip on the objects. HS1 received frequency-modulated intensity encoding on 6 electrodes with no jitter.

HS2 performed a subset of virtual Jebsen Hand Function Test (JHFT), Activities Measures for Upper Limb Amputees (AM-ULA), and custom tasks with the vLA in velocity-control [22]. [23] in 3 separate experiments. The subset of tasks included 1) moving a light and a heavy can from a starting location to a target location, 2) picking up a marble and placing it within a cup, 3) pouring the marble from the cup into a bowl, 4) picking up a spoon and scooping the marble from the bowl back into the cup, 5) picking up a key and unlocking a lock, 6) turning a doorknob, 7) stacking checkers, and 8) pretend writing. Tasks 1, 2, 4, 7, and 8 were JHFT subtasks [22]. Tasks 3, 4, 5, 6, and 8 were AM-ULA subtasks [23]. HS2 performed each subtask twice in a row during a single ADL assessment. A single presentation of the subtask had sensory feedback enabled, whereas the other



Fig. 2. HS2 performing the texture identification task. Corrugated

60

did not. Whether or not stimulation occurred in the first presentation was randomly decided on a 50/50 probability. The volunteer was given 60 s to complete the presentation of the ADL subtask before a timeout occurred. The volunteer controlled the vLA in 6-DOF velocity control on all days. The volunteer also completed physical versions of the marble moving, checkers, and writing tasks with the modified Ada Hand with the thumb, index, middle, ring, and little DOFs in velocity mode. Sensory feedback calibration was variable, where we used frequency- and/or amplitude-modulated intensity encoding through 2 or 3 electrodes with or without jitter.

To determine whether the presence of sensory feedback affected overall task performance, we performed t-tests on the time needed to complete the tasks where successful runs occurred in both the stimulation-on and stimulation-off groups. T-tests were paired if the number of successful stimulation on and off runs were the same, and two-sample t-tests if the number of runs differed.

Because sensory feedback and the imminent motor task can guide motor performance with physical prosthetic devices [5], [24], [25], we investigated sensor activity during HS2's ADL tasks in an attempt to distinguish how sensory feedback and task-related motor demands affected volunteer-object interactions. Due to the freeform nature of the experiment, all VPH-object interactions were reliant on the volunteer's manipulations of the VPH. Consequently, assessing the sensor activity allowed us to indirectly assess VPH motor performance and also to examine whether differences in motor performance affected sensory experiences via closed-loop bidirectional interactions. Using MuJoCo's detailed virtual data logs that record all VPH activity, we compiled sensor output mean amplitude and above-zero duration during every trial in separate ANOVAs. Both ANOVAs were grouped by the presence (or absence) of stimulation, the contact sensor location, and the subtask. A sensor's data were included only if the sensor was tied to USEA stimulation for half of the trials as described above in order to investigate differences caused by the presence or absence of intraneural microstimulation. All other sensor logs were not included. We removed outliers before performing the ANOVAs. An outlier was defined as having a value outside of the bounds set by 3 median absolute deviations from the overall median. We performed post-hoc Fisher's least significant difference (LSD) procedures within the groups that showed significant differences in the ANOVAs in order to identify the factors that contributed to the differences identified in the ANOVAs.

III. RESULTS

A. Open-loop Sensory Task

We examined HS2's ability to identify the stimuli's receptive field, intensity, the receptive field and intensity simultaneously on each day, and the overall ability to identify both the receptive field and intensity simultaneously for every trial across both days, leading to a total number of 7 multiple comparisons. At the familywise error rate of $\alpha = 0.05$, the volunteer successfully identified the stimuli's receptive field on both days, and he identified the receptive field and intensity simultaneously on each day individually and both days combined. The subject

identified the intensity of the stimuli on the second day, but he did not identify the intensity on the first day (p = 0.4306). Confusion matrices for the results from these tests can be seen in Fig. 3 (receptive fields) and Fig. 4 (intensities).

B. Size and Compliance Identification

Our closed-loop system allowed for both human volunteers to identify virtual object properties. Given that S1's test involved proprioceptive USEA stimulation that caused feedback even when no contact was made, we investigated whether he could identify the presence or absence of a cylinder from virtual contact. We also sought to determine whether he could identify the object presented to him, leading to 2 comparisons at familywise $\alpha=0.05$. The volunteer identified the presence of an object and the objects' size with statistical significance.

For the size/compliance identification tasks, we investigated HS2's ability to recognize size, compliance, and combined size and compliance, leading to 3 multiple comparisons at a familywise error rate of $\alpha = 0.05$ each for the virtual 2x2,

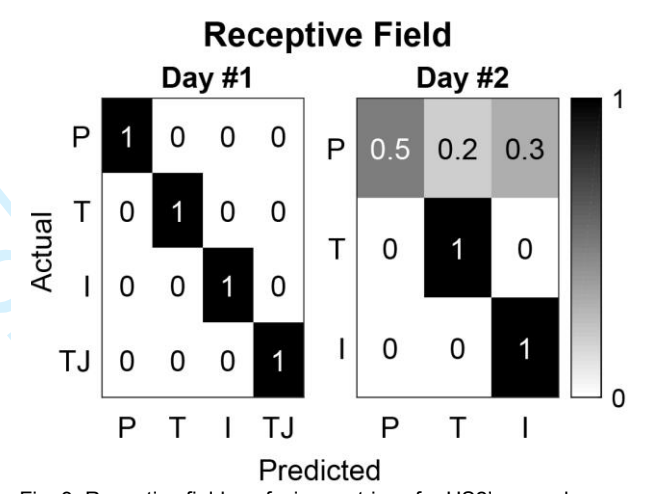


Fig. 3. Receptive field confusion matrices for HS2's open-loop sensory task. P = palm contact, T = thumb contact, I = index contact, and TJ = thumb joint. The volunteer correctly identified the receptive field of the stimuli on both days (*p*'s < 0.0001).

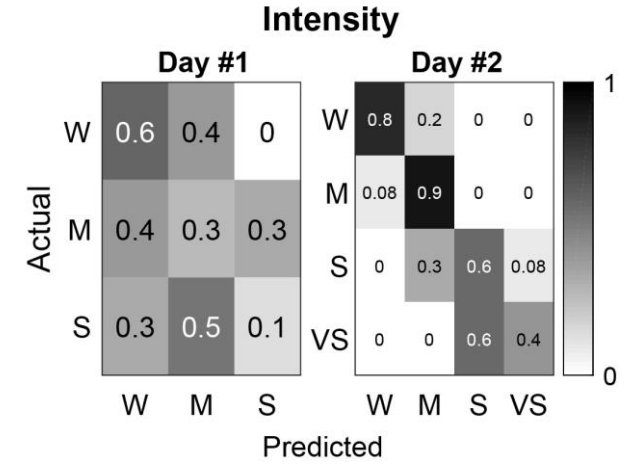


Fig. 4. Intensity confusion matrices for HS2's open-loop sensory task. W = weak, M = medium, S = strong, and VS = very strong. The volunteer was unable to identify the intensity on Day #1 (p = 0.4306), but was able to identify the intensity on Day #2 (p < 0.0001).

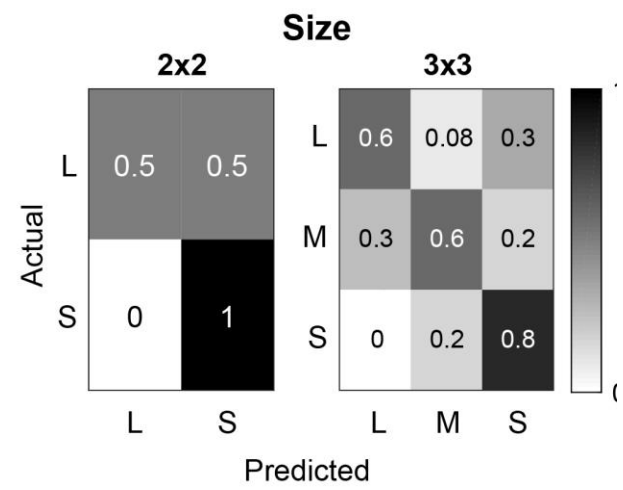


Fig. 5: Size confusion matrices for HS2's size and compliance identification task. L = large, M = medium, and S = small. The volunteer was able to identify the size during both experiments (2x2 p = 0.0106, 3x3 p < 0.0001).

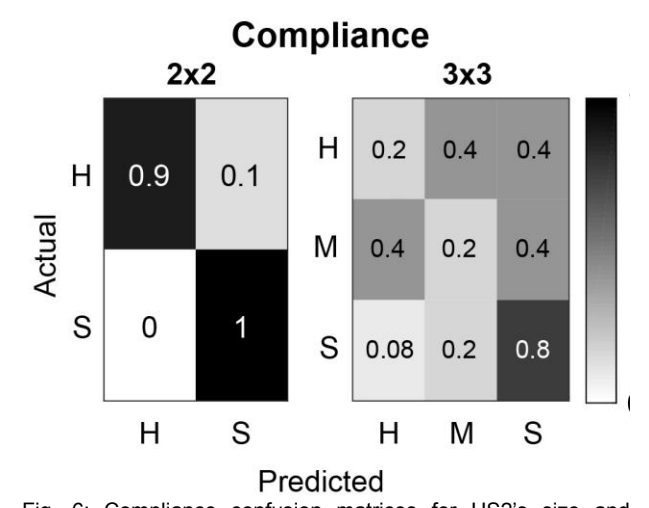


Fig. 6: Compliance confusion matrices for HS2's size and compliance identification task. H = hard, M = medium, and S = soft. The volunteer was able to identify compliance during the 2x2 experiment (ρ < 0.0001), but he was unable to do so during the 3x3 experiment (ρ = 0.2933).

virtual 3x3, and for the physical 2x2 experiments. HS2 identified all object properties with statistical significance except for the compliance in the virtual 3x3 experiment (p = 0.2933) and size in the physical 2x2 experiment (p = 0.2272). Confusion matrices for the results from the virtual tests can be seen in Fig. 5 (sizes) and Fig. 6 (compliances).

C. Texture Identification

The volunteer correctly identified the texture of the wall he stroked as either "smooth" or "rough," both with motor control of the vLA disabled (11/12 correct) and with motor control enabled (12/12 correct). These individual experiments and combined results were analyzed and controlled for 3 multiple comparisons at a familywise error rate of $\alpha=0.05$. The volunteer identified texture with statistical significance in all 3 comparisons.

D. ADL Tasks

Transactions on Neural Systems and Rehabilitation Engineering

HS1 successfully completed several door-opening tasks with closed-loop control. This was the first time a human volunteer used a prosthetic under voluntary motor control with contact-mediated USEA stimulation evoking percepts on a phantom hand. During this pilot session, we invited the volunteer to act freely within the VRE, knowing he had closed-loop control of the VPH. Almost immediately, the volunteer stroked the virtual door with the VPH, gasped, and remarked, "Oh my God, I just felt that door" (see supplementary video S3). After continuing to stroke the virtual door, he exclaimed, "God, that is so cool!" Previous open-loop stimulation through the same and different USEA electrodes had not evoked a comparable reaction. Following the pilot exploration period, the volunteer was able to remove a latch, grab a handle, and open a door. The volunteer was also able to grab a door handle, rotate it, and pull a door open.

HS1 successfully completed several ARAT tasks with closed-loop control of the vMPL. The volunteer successfully lifted the 2-cm cube, 4-cm cube, and grinding stone from the table surface to the top of the shelf. He successfully picked up a cylindrical glass and poured its contents into a stationary glass. The volunteer removed a cricket ball from a stationary bowl and placed it into another stationary bowl on top of the shelf. The volunteer was unable to pick up a 10-cm cube on the table, a ball-bearing in a stationary bowl, or a hollow tube from a pedestal.

HS2 completed a total of 4 modified JHFT and custom ADL tasks under a 60-s time limit with the vLA (Table 1). In brief, the volunteer was able to pick up a small ball and drop it into a pitcher, pour a small ball from a pitcher into a bowl, turn a virtual door knob, and pretend write. The volunteer was unable to move both cans, use a spoon to scoop a small ball out of a bowl and drop it into a pitcher, stack 3 checkers on top of one another, or use a key in a lock.

To examine the potential consequences of sensory feedback on task performance, stimulation controlled by sensor activation was delivered via USEA electrodes on 50% of the trials; in the other 50% of trials, stimulation was not delivered regardless of sensor output. The presence or absence of stimulation did not affect the time it took for HS2 to complete tasks 3, 6, or 8, which were the tasks that had successful runs in both the stimulation-on and stimulation-off conditions (#3, p =

TABLE 1 HS2 Successful ADL Results

ADL Task	Stimulation	Success/total	Time (s)
Move marble*	No	1/4	31
Pour pitcher ⁺	No	4/4	28.5 20
	Yes	4/4	29.5 13
Door	No	4/4	24.5 33
knob⁺	Yes	1/4	32 21
Pretend write*+	No	1/4	14
	Yes	2/4	25.5 33

Table 1. Results of successful virtual ADL tasks by HS2. Time is reported as median | IQR for testing groups with multiple successes. * = JHFT subtask. + = AM-ULA subtask.

Kluger et al.: Virtual Reality Provides an Effective, Low-cost Platform for Evaluating Closed-loop Neuromyoelectric Prosthetic Hands

2

3

4

5

6

7

8

9

10

11

12

13

14

15

16

17

18

19

20

21

22

23

24

25

26

27

28

29

30

31

32

33

34

35

36

37

38

39

40

41

42

43

44

45

46

47

48

49

50

51

52

53

54

55

56

57

58 59

60

0.4437; #6, p = 0.9812; #8 p = 0.7564; unpaired t-tests). When using the Ada Hand in the physical-world tests under a 60-s trial limit, the volunteer performed the marble-moving task 6 out of 6 tries, the checkers task 4 out of 6 tries, and wrote with a pen 2 out of 2 tries.

If stimulation affected motor performance, then changes in motor behaviors in turn might have affected the intensity or duration of sensor activation, thereby demonstrating bidirectional closed-loop sensorimotor interactions. Consistent with this hypothesis, the mean intensity of sensor activation during contact was greater on trials for which stimulation was on (mean \pm SEM: 26.82 \pm 4.32 N) than on trials for which stimulation was off (19.56 \pm 3.17 N; $F_{1.68} = 5.52$, p = 0.0261) (Fig. 7a). These results indicate that the subject handled the object more firmly when sensory feedback was provided, which in turn affected the sensory feedback he received. Mean sensor amplitude also differed significantly by sensor location ($F_{1.68}$ = 5.59, p = 0.0240), where the LSD post-hoc tests showed greater activation from the index finger (48.53 \pm 6.14 N) relative to the palm (14.77 \pm 2.07 N), middle finger (28.46 \pm 1.26 N), and ring finger (13.17 \pm 2.13 N), and between the ring and middle fingers (p's < 0.05) (Fig. 7b). These results indicate that the volunteer's grasps differentially activated different sensors, possibly because he differentially activated the various independent degrees of freedom associated with these sensors. Sensor output amplitude did not differ significantly by task (Fig. 7c), or by any combination of the presence of stimulation, sensor location, and task (p's > 0.05).

The duration of sensor activation showed a statistical trend $(F_{1,78} = 3.20, p = 0.0819)$ to be shorter for stimulation-on trials $(10.23 \pm 1.24 \text{ s})$ than for stimulation-off trials $(12.69 \pm 1.54 \text{ s})$, indicating a tendency to handle the objects more quickly when sensory feedback was provided (Fig. 7a). The duration varied significantly by sensor location ($F_{3.79} = 10.15$, p = 0.0001), where a post-hoc test showed the duration on the middle finger $(4.13 \pm 0.19 \text{ s})$ was shorter than on the other three sensors (palm: 14.77 ± 2.07 s; index: 10.32 ± 1.70 s; 4.13 ± 0.77 s; ring: 14.08 ± 1.76 s; p's < 0.05), once again indicating that the volunteer's grasping movements produced differential activation of sensors in different locations (Fig. 7b). Contact duration also varied by subtask ($F_{7,78} = 3.71$, p = 0.0040), where the LSD post-hoc tests showed the durations during the spoon task (task #4, 21.05 ± 1.09 s) were significantly longer than on any other task (#1: 8.46 ± 2.04 s; #2: 9.32 ± 2.32 s; #3: $8.02 \pm$ 1.56 s; #5 $13.58 \pm 3.17 \text{ s}$; #6 $6.84 \pm 1.42 \text{ s}$; #7 $10.94 \pm 3.51 \text{ s}$; #8: 13.53 ± 2.02 s), the key task (#5) had longer durations than the door knob task (#6), and the writing task (#8) had longer durations than the door knob task (p's < 0.05) (Fig. 7c). The variability in durations suggests that the subject used the VPH differently across different subtasks. The duration of sensor activation did not show any statistically significant differences for any interactions of the task, presence of stimulation, and sensor location (p's > 0.05).

IV. DISCUSSION

Our findings support the use of VREs for assessing the ability to identify virtual object properties. They further suggest conducting closed-loop object identification tests in a VRE may

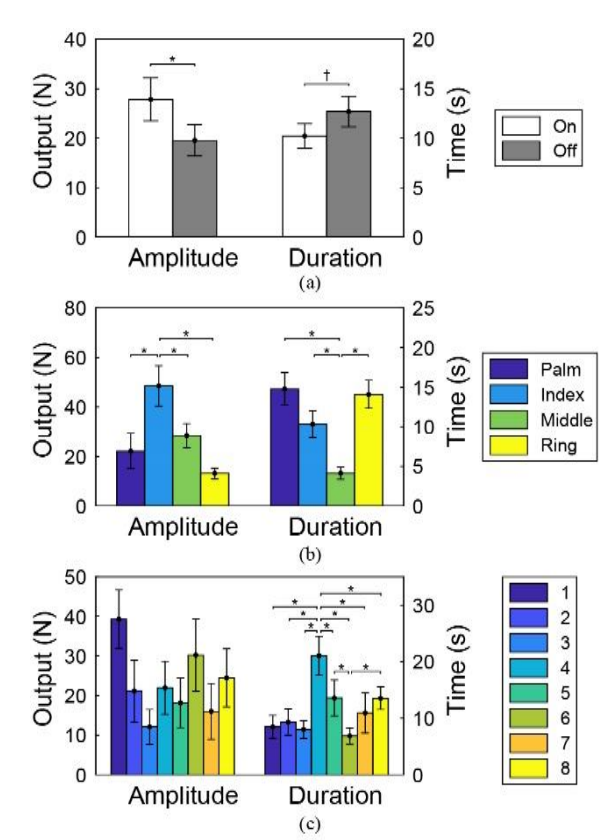


Fig. 7: Sensor output during S2's ADL tasks. Differences in sensor activity were observed due to the presence of stimulation (A), the sensor location (B), and the ADL subtask (C). * = p < 0.05; † = p <

be in some ways superior to testing in a physical world scenario. Complex virtual ADL tasks requiring subtle manipulations of a VPH, like virtual copies of the ARAT, JHFT, and AM-ULA, are possible, but are very challenging. A lack of proficiency in these virtual tasks may not be indicative of real-world prosthetic capabilities. Furthermore, we were able to use the VRE to show indications of bidirectional sensorimotor influences of closedloop prosthetic arm control.

A. Open-loop Sensory Task

HS2 successfully identified the stimuli's receptive field and intensity simultaneously, which adds credence to USEAmediated sensory feedback. These results corroborate findings previous studies demonstrating that microstimulation was capable of evoking graded and locationspecific perceptions on human amputees' phantom hands [6], [7].

The volunteer's inability to identify the intensity on Day #1 of open-loop testing, but an ability to do so on Day #2, may be a consequence of one or several physiological phenomena that were not tested for in a systematic manner. One possible explanation is that a learning effect had taken place, in which the subject was not used to the stimuli presentations on experiment Day #1, but he may have become better trained to identify the differences in stimulation intensity by experiment Day #2, which were 97 days apart. This difference could be partly explained by cortical reorganization effects, where cortical reorganization following his injury several years prior

was subsequently reversed following the influx of afferent input to his central nervous system through USEA stimulation [26]–[28], differences between the efficacy of rate and population encoding in the peripheral nervous system [29]–[31], and/or differences in the modalities of information being conveyed to the central nervous system due to activation of different afferent fibers.

B. Virtual vs. Physical Prosthesis Performance

We have demonstrated that VPHs can be used to predict performance of a physical prosthesis for object identification tasks, and these tasks may be advantageously performed in a VRE as opposed to a physical environment. However, the inability to perform some tasks in a VRE does not necessarily predict the same lack of abilities with a physical prosthesis.

1) Object identification: VREs are a powerful tool for assessing amputees' object-identifying capabilities using prosthetic hands with closed-loop capabilities. Both volunteers were able to identify object properties in all of the virtual and physical object identification tasks presented to them, including texture, size, compliance, and simultaneous size and compliance. The only object properties that were not successfully identified in our testing was size in the physical 2x2 size/compliance task and compliance in the 3x3 virtual size/compliance task. However, the inability to identify compliance in the 3x3 test may have been from a simulation error that we subsequently identified: Index finger contact with hard objects resulted in a substantial oscillating sensor output, which does represent a challenge for closed-loop VRE testing where modelled physical behavior must be diligently bugchecked before testing.

Identification testing using physical objects introduced secondary cue confounds to the object identification tasks, another problem that VRE-testing completely eliminated. Because the VPH's motors were silent, the volunteer could not hear when the motors would stall when contacting an object as he could with the physical Ada Hand. We attempted to eliminate auditory cues by applying earmuffs to the volunteer during physical testing. Furthermore, a physical world analogue of the texture identification test also involves secondary cues, some of which also are eliminated by the use of the VRE. A physical wall-stroking test inevitably results in an amputee subject receiving secondary cues through skin-socket interactions, which cannot occur with a VPH. Furthermore, the VPH eliminated experimenter error where objects could be presented with a regularity that would have been difficult to achieve in the physical test. This regularity may have been the determining factor that allowed the volunteer to identify size in the virtual tasks, but not in the physical task. Thus, due to its ability to eliminate certain secondary cues and experimenter errors, testing closed-loop object discrimination in VREs may be superior in multiple ways to testing in the physical world.

2) ADLs: The volunteers successfully completed several virtual and physical ADL tasks. Even though the volunteer was able to perform ADL tasks in the VRE, comparing the results from virtual performance to physical performance suggests virtual ADLs are often more difficult than the physical tests they are modelled after. HS2 was able to complete the checker stacking task in the physical world 4 out of 6 times but was never able to do so in the virtual task. Furthermore, he

completed the marble moving task in the physical world 100% of the time, but was able to do this task only 1 time out of 8 tries in the virtual tests. Although the vLA was not a replica of the physical Ada Hand, these results suggest complex ADL tasks are much easier to perform in the physical world than in a VRE with a VPH, and VRE testing of ADLs may be a poor indicator of physical ADL performance with socket-mounted prostheses.

C. Using VPHs for Amputee Behavior Analyses

VREs are a useful tool for assessing subtle VPH behaviors when exposing amputees to complex tasks, which suits using VREs for identifying changes in sensorimotor behaviors resulting from the presence or absence of sensory feedback. A lack of improvement in ADLs from closed-loop control could be due to virtual ADL difficulty.

1) Sensory feedback's impact on virtual performance: Sensory feedback influenced subjects' performance on several but not all metrics.

The volunteer generated more force on the sensors tied to USEA stimulation during trials when sensor-driven USEA-evoked sensory feedback was provided than when this intraneural microstimulation was absent. The VPH sensors could be activated only by the movements of the VPH that were controlled by the volunteer. Consequently, these results indicate that it was the volunteer himself who generated more forces on the VPH when sensory feedback was applied. This change in motor behavior could have been due to simple enjoyment of the evoked sensation; alternatively, the volunteer may have generated more force when tactile feedback let him know that contact had been properly initialized.

HS2's virtual experiments demonstrate that he was executing different grasps and movements: sensor output amplitude varied by sensor location, and the duration of sensor activation varied by task and sensor. These findings suggest the volunteer used the VPH in grip- and task-specific ways in an attempt to complete the goal presented to him.

Results from both ANOVAs indicate grip- and task-specific VPH interactions. The index finger's sensor had the highest mean amplitude of the 4 sensors that were analyzed, which coincides with results from an isometric gripping study which found that the index finger produced the highest forces of the index, middle, and ring fingers [32]. Presumably, the volunteer used the highest forces on this finger due to remnant gripping behaviors from before his amputation-causing injury. The ring finger had the lower amplitudes relative to the index and middle fingers due to the fact that its usage was predominantly incorporated for power grips, a grip type where normal forces were distributed across a wide surface area. The middle finger experienced intermittent contact with objects in a power grip, due to it being the longest finger, and it experiences a lack of touch events during two-finger pinch grips, thus its lower mean duration compared with the other sensors. Furthermore, the middle finger was not intentionally used in pinch grips, so contact during these tasks was likely accidental and very shortlived. For task-wise sensor activity, we observed the highest durations in the spoon task. HS2 readily achieved a prolonged power grip on the spoon, but had difficulty using the spoon to scoop up the ball, thus the prolonged contact. Similarly, the knob task showed shorter durations than the writing and key tasks. The volunteer was able to turn the knob by resting his

60

fingers on the end of the knob and sliding the whole hand across the side with relative ease, leading to the low contact durations. The writing task, like the spoon task, allowed for prolonged power grips around the target object, which caused long contact durations. The key task was exceedingly difficult, causing the key to be frequently dropped, leading to short contact durations.

2) Virtual ADLs did not improve with sensory feedback: Although USEA-evoked sensory feedback allowed for object identification, feedback did not improve the ability to perform virtual ADLs. This combination of results is similar to a previous finding that sensory feedback allowed for identification of the presence or absence of a block between a sensorized prosthetic hand's fingers (much like HS1's identification task), but did not improve one subject's ability to perform the Southampton Hand Assessment Procedure [33]. However, this previous finding was from a single subject within one study, and was unique among the documented literature. The present results extend these previous results.

The absence of an effect of sensory feedback on HS2's motor performance is contrary to most observations that sensory feedback to the nervous system improves motor performance [24], [34], [35]. The small number of trials, task difficulty, and/or the tasks not being tailored to demonstrate sensory benefits may be contributing factors.

The lack of improvement from cutaneous sensory feedback may have arisen from the lack of supporting proprioceptive feedback associated VPH motor activity, where both endogenous and USEA-mediated exogenous feedback were totally absent due to our use of velocity control and inability to excite proprioceptive afferents, respectively. Cutaneous feedback alone does not create kinesthesia, or the knowledge of joint position that proprioceptive feedback generates [34], which has been demonstrably useful in closed-loop tasks [6], [19]. The cutaneous stimuli we provided were not applied to encode skin stretch, where skin stretch sensations have been shown to produce kinesthesia [36], [37].

3) Abstract effects of VPH interaction: We observed several phenomena that promote the incorporation of intuitive sensory feedback into prosthetic limbs, beyond the object identification capabilities previously described. When HS1 first touched and felt the virtual door with his VPH under his own volition, it resulted in a startle response ("Oh, my God!") that differed qualitatively from his response to previous open-loop stimulation through the same and different USEA electrodes. The different types of responses evoked by open-loop and closed-loop stimulation further reinforce the functional consequences and bidirectional interactions of sensorimotor closed-loop neuroprostheses. Subjective differences in sensory perception may in part arise from differences in cortical activation, as suggested by electrophysiological responses recorded in cortex of non-human primates [38]. The virtual ADL sensor output results demonstrate the functional consequences and ongoing interactive nature of bidirectional sensorimotor communication. Not only do the results from both experiments indicate that sensory feedback guided motor performance, but also changes in motor performance in turn influenced the evoked perception due the sensory stimulation that the volunteer received.

The volunteer's elation of his virtual interaction with the door and word usage ("I just touched that door!") also suggests that HS1 embodied the VPH to at least some degree. In previous work, applying sensory feedback to physical prosthetic devices has demonstrated quantifiably greater embodiment of the prosthetic device [39]. This result promotes further investigation into what degree of embodiment is possible with VPHs. The elation expressed by the volunteer ("...that is so cool!") further demonstrates the emotional benefit of adding sensory feedback to a prosthetic hand. The behavioral, emotional, and rehabilitational influences of closed-loop control of prosthesis-driven sensory feedback also demands more attention in future work investigating closed-loop control of prosthetic hands, both virtual and physical.

V. CONCLUSION

We have demonstrated that the use of intramuscular EMG implants and intraneural USEAs allows for closed-loop control of VPHs, and that real-time, bidirectional sensorimotor communication provides measurable functional benefits for prostheses. Several closed-loop virtual tasks were executed by human amputees. Our volunteers were also able to identify object properties such as size, compliance, and texture and complete virtual ADLs. These promising results promote further investigation of these closed-loop control methods with a physical limb mounted to the residual limb of a transradial amputee. This work supports the hypothesis that experimental results from using VPHs within VREs may serve as preliminary validation of their closed-loop control methods when they are translated to physical limbs. The use of VPHs within VREs can be superior to the use of a physical limb for testing closed-loop object discrimination capabilities due to the highly repeatable presentation of objects and elimination of secondary sensory cues. However, use of VREs in virtual ADL assessments may not always accurately predict real-world performance with physical prostheses. Finally, we have provided evidence that complements published literature documenting bidirectional sensorimotor influences during primate reaching and grasping tasks.

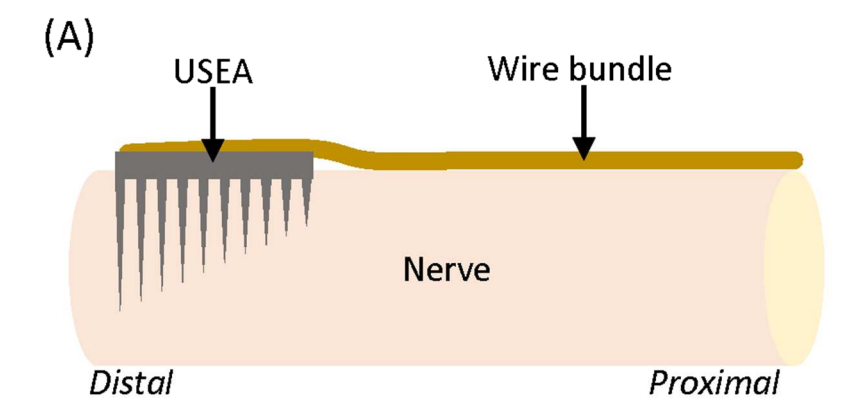
REFERENCES

- E. Biddiss and T. Chau, "Upper-limb prosthetics: critical factors in device abandonment," Am. J. Phys. Med. Rehabil., vol. 86, no. 12, pp. 977–987, Dec. 2007.
- [2] P. F. Pasquina et al., "First-in-Man Demonstration of Fully Implanted Myoelectric Sensors for Control of an Advanced Electromechanical Arm by Transradial Amputees," J. Neurosci. Methods, vol. 244, pp. 85– 93, Apr. 2015.
- [3] M. Ortiz-Catalan, R. Brånemark, B. Håkansson, and J. Delbeke, "On the viability of implantable electrodes for the natural control of artificial limbs: Review and discussion," *Biomed. Eng. OnLine*, vol. 11, p. 33, Jun. 2012.
- [4] L. H. Smith, T. A. Kuiken, and L. J. Hargrove, "Real-time simultaneous and proportional myoelectric control using intramuscular EMG," *J. Neural Eng.*, vol. 11, no. 6, p. 066013, Dec. 2014.
- [5] D. W. Tan, M. A. Schiefer, M. W. Keith, J. R. Anderson, J. Tyler, and D. J. Tyler, "A neural interface provides long-term stable natural touch perception," *Sci. Transl. Med.*, vol. 6, no. 257, p. 257ra138, Oct. 2014.
- [6] S. Wendelken et al., "Restoration of motor control and proprioceptive and cutaneous sensation in humans with prior upper-limb amputation via multiple Utah Slanted Electrode Arrays (USEAs) implanted in

60

- residual peripheral arm nerves," *J. NeuroEngineering Rehabil.*, vol. 14, Nov. 2017
- [7] G. A. Clark et al., "Using multiple high-count electrode arrays in human median and ulnar nerves to restore sensorimotor function after previous transradial amputation of the hand," in 2014 36th Annual International Conference of the IEEE Engineering in Medicine and Biology Society, 2014, pp. 1977–1980.
- [8] N. M. Ledbetter et al., "Intrafascicular stimulation of monkey arm nerves evokes coordinated grasp and sensory responses," J. Neurophysiol., vol. 109, no. 2, pp. 580–590, Jan. 2013.
- J. Diaz, "Lauderdale woman appreciates every movement of her hightech hand - Sun Sentinel," Sun Sentinel. [Online]. Available: http://www.sun-sentinel.com/features/fl-bionic-hand-woman-20150807story.html. [Accessed: 12-Feb-2018].
- [10] A. Saenz, "Deka's Luke Arm In Clinical Trials, Is it the Future of Prosthetics? (Video)," Singularity Hub, 01-Dec-2009.
- [11] E. Todorov, T. Erez, and Y. Tassa, "MuJoCo: A physics engine for model-based control," in 2012 IEEE/RSJ International Conference on Intelligent Robots and Systems, 2012, pp. 5026–5033.
- [12] M. Hauschild, R. Davoodi, and G. E. Loeb, "A virtual reality environment for designing and fitting neural prosthetic limbs," *IEEE Trans. Neural Syst. Rehabil. Eng. Publ. IEEE Eng. Med. Biol. Soc.*, vol. 15, no. 1, pp. 9–15, Mar. 2007.
- [13] J. M. Lambrecht, C. L. Pulliam, and R. F. Kirsch, "Virtual reality environment for simulating tasks with a myoelectric prosthesis: an assessment and training tool," *J. Prosthet. Orthot. JPO*, vol. 23, no. 2, pp. 89–94, Apr. 2011.
- [14] D. Putrino, Y. T. Wong, A. Weiss, and B. Pesaran, "A training platform for many-dimensional prosthetic devices using a virtual reality environment," *J. Neurosci. Methods*, vol. 244, pp. 68–77, Apr. 2015.
- [15] A. Branner, R. B. Stein, and R. A. Normann, "Selective Stimulation of Cat Sciatic Nerve Using an Array of Varying-Length Microelectrodes," *J. Neurophysiol.*, vol. 85, no. 4, pp. 1585–1594, Apr. 2001.
- [16] J. A. George, M. R. Brinton, C. C. Duncan, D. T. Hutchinson, and G. A. Clark, "Improved Training Paradigms and Motor-decode Algorithms: Results from Intact Individuals and a Recent Transradial Amputee with Prior Complex Regional Pain Syndrome," presented at the 40th International Engineering in Medicine and Biology Conference, Honolulu, HI, 2018.
- [17] D. M. Page et al., "Motor Control and Sensory Feedback Enhance Prosthesis Embodiment and Reduce Phantom Pain after Long-term Hand Amputation," Front. Hum. Neurosci., vol. (In review), Jan. 2018.
- [18] S. Wendelken et al., "Partial Restoration of Sensorimotor Function After Hand Amputation Using Multiple Electrode Arrays," in Proceedings of the IEEE Biomedical Engineering Society Annual Meeting, 2014, San Antonio, TX, 2014.
- [19] T. S. Davis et al., "Restoring motor control and sensory feedback in people with upper extremity amputations using arrays of 96 microelectrodes implanted in the median and ulnar nerves," *J. Neural Eng.*, vol. 13, no. 3, p. 036001, Jun. 2016.
- [20] E. L. Graczyk, B. P. Delhaye, M. A. Schiefer, S. J. Bensmaia, and D. J. Tyler, "Sensory adaptation to electrical stimulation of the somatosensory nerves," *J. Neural Eng.*, vol. 15, no. 4, p. 046002, 2018.
- [21] R. C. Lyle, "A performance test for assessment of upper limb function in physical rehabilitation treatment and research," *Int. J. Rehabil. Res. Int. Z. Rehabil. Rev. Int. Rech. Readaptation*, vol. 4, no. 4, pp. 483–492, 1981.
- [22] R. H. Jebsen, N. Taylor, R. B. Trieschmann, M. J. Trotter, and L. A. Howard, "An objective and standardized test of hand function," *Arch. Phys. Med. Rehabil.*, vol. 50, no. 6, pp. 311–319, Jun. 1969.
- [23] L. Resnik et al., "Development and Evaluation of the Activities Measure for Upper Limb Amputees," Arch. Phys. Med. Rehabil., vol. 94, no. 3, pp. 488-494.e4, Mar. 2013.
- [24] G. S. Dhillon and K. W. Horch, "Direct neural sensory feedback and control of a prosthetic arm," *IEEE Trans. Neural Syst. Rehabil. Eng. Publ. IEEE Eng. Med. Biol. Soc.*, vol. 13, no. 4, pp. 468–472, Dec. 2005
- [25] J. Diedrichsen, R. Shadmehr, and R. B. Ivry, "The coordination of movement: optimal feedback control and beyond," *Trends Cogn. Sci.*, vol. 14, no. 1, pp. 31–39, Jan. 2010.
- [26] T. Allard, S. A. Clark, W. M. Jenkins, and M. M. Merzenich, "Reorganization of somatosensory area 3b representations in adult owl monkeys after digital syndactyly," *J. Neurophysiol.*, vol. 66, no. 3, pp. 1048–1058, Sep. 1991.

- [27] W. Gaetz et al., "Massive cortical reorganization is reversible following bilateral transplants of the hands: evidence from the first successful bilateral pediatric hand transplant patient," Ann. Clin. Transl. Neurol., vol. 5, no. 1, pp. 92–97, Dec. 2017.
- [28] J. Yao, A. Chen, T. Kuiken, C. Carmona, and J. Dewald, "Sensory cortical re-mapping following upper-limb amputation and subsequent targeted reinnervation: A case report," *NeuroImage Clin.*, vol. 8, pp. 329–336, Jan. 2015.
- [29] M. A. Muniak, S. Ray, S. S. Hsiao, J. F. Dammann, and S. J. Bensmaia, "The Neural Coding of Stimulus Intensity: Linking the Population Response of Mechanoreceptive Afferents with Psychophysical Behavior," *J. Neurosci.*, vol. 27, no. 43, pp. 11687–11699, Oct. 2007.
- [30] E. L. Graczyk, M. A. Schiefer, H. P. Saal, B. P. Delhaye, S. J. Bensmaia, and D. J. Tyler, "The neural basis of perceived intensity in natural and artificial touch," *Sci. Transl. Med.*, vol. 8, no. 362, p. 362ra142, Oct. 2016.
- [31] C. C. McIntyre, A. G. Richardson, and W. M. Grill, "Modeling the excitability of mammalian nerve fibers: influence of afterpotentials on the recovery cycle," *J. Neurophysiol.*, vol. 87, no. 2, pp. 995–1006, Feb. 2002
- [32] E. Y. Chao, J. D. Opgrande, and F. E. Axmear, "Three-dimensional force analysis of finger joints in selected isometric hand functions," *J. Biomech.*, vol. 9, no. 6, pp. 387–396, 1976.
- [33] M. Schiefer, D. Tan, S. M. Sidek, and D. J. Tyler, "Sensory feedback by peripheral nerve stimulation improves task performance in individuals with upper limb loss using a myoelectric prosthesis," *J. Neural Eng.*, vol. 13, no. 1, p. 016001, Feb. 2016.
- [34] P. D. Marasco et al., "Illusory movement perception improves motor control for prosthetic hands," Sci. Transl. Med., vol. 10, no. 432, p. eaao6990, Mar. 2018.
- [35] M. C. Dadarlat, J. E. O'Doherty, and P. N. Sabes, "A learning–based approach to artificial sensory feedback leads to optimal integration," *Nat. Neurosci.*, vol. 18, no. 1, pp. 138–144, Jan. 2015.
- [36] B. B. Edin and N. Johansson, "Skin strain patterns provide kinaesthetic information to the human central nervous system," *J. Physiol.*, vol. 487, no. 1, pp. 243–251, Aug. 1995.
- [37] D. F. Collins, K. M. Refshauge, G. Todd, and S. C. Gandevia, "Cutaneous Receptors Contribute to Kinesthesia at the Index Finger, Elbow, and Knee," *J. Neurophysiol.*, vol. 94, no. 3, pp. 1699–1706, Sep. 2005
- [38] J. Chen, S. D. Reitzen, J. B. Kohlenstein, and E. P. Gardner, "Neural Representation of Hand Kinematics During Prehension in Posterior Parietal Cortex of the Macaque Monkey," *J. Neurophysiol.*, vol. 102, no. 6, pp. 3310–3328, Dec. 2009.
- [39] P. D. Marasco, K. Kim, J. E. Colgate, M. A. Peshkin, and T. A. Kuiken, "Robotic touch shifts perception of embodiment to a prosthesis in targeted reinnervation amputees," *Brain*, vol. 134, no. 3, pp. 747–758, Mar. 2011.



(B)

91	92	93	94	95	96	97	98	99	100
81	82	83	84	85	86	87	88	89	90
71	72	73	74	75	76	77	78	79	80
61	62	63	64	65	66	67	68	69	70
51	52	53	54	55	56	57	58	59	60
41	42	43	44	45	46	47	48	49	50
31	32	33	34	35	36	37	38	39	40
21	22	23	24	25	26	27	28	29	30
11	12	13	14	15	16	17	18	19	20
1	2	3	4	5	6	7	8	9	10

82x114mm (300 x 300 DPI)

TABLE S2 Stimulation Settings for Virtual Tasks

	Stimulation		for Virtual T	asks		
Task	Sensor	Electrode	Amp. (μA)	Freq. (Hz)	Jitter	
		HS1				
	Ring Joint	u25	74	1-200		
	Ring Joint	u74	100	1-200		
Size ID	Middle distal	m18	50	100	No	
	Ring distal	m48	20	100		
	Little distal	u5	100	100		
Door Tasks	Middledistal	m66	25	1-100	No	
	Ringjoin	m25	80	1-333		
	Ringjoint	m74	100	1-333		
ARAT	Middle distal	m68	100	150-500	No	
ARAT	Ring distal	m18	50	10-100	NO	
	Ring distal	m48	20	10-100		
	Little distal	m5	100	10-100		
		HS2				
	Palm lateral	u72	100	50-200		
Open-loop	Index distal	m3	13	10-200	Yes	
#1	Thumb distal	m15	100	10-200		
	Thumb joint	m38	40	10-300		
	Palm lateral	m73	10-45	100		
Open-loop	Index distal	m47,m57	25-55	20	Yes	
#2	Thumb distal	m39	30-70	20		
Texture	Middle distal	m67	0-18	10-150	Yes	
S/C 2x2	Middle distal	m3	0-10	10-300	Yes	
	Middle distal	m61	0-60	10-300		
S/C3x3 #1	Index distal	m27	40-100	30-100	Yes	
S/C#2	Index distal	m47	30-50	10-65	No	
S/C Phys.	Middle distal	m46	10-30	40-70	No	
,,	Thumb distal	m17	0-31	10-200		
ADL#1	Middle distal	m36	0-20	10-200	No	
	Palm medial	m79	0-30	10-200		
ADL#2	Ring distal	m37	0-90	10-300	Yes	
	Middle distal	m61	0-40	10-300		
	Palm lateral	m67	0-50	10-300		
ADL#3	Index distal	m47	30-47	30	No	
	Ring distal	m54	40-65	30		
ADL Phys.	Index distal	m46	35	10-100	Yes	
	Middle distal	u41,u53	70	10-100		

88x177mm (96 x 96 DPI)

Fig. S1. (A) Diagram showing the side view of a USA on an implanted nerves, where the long electrodes are on the distal end of the implants. (B) Back-plane view of the implanted USEA with an electrode numbering schematic. Shaded boxes indicate reference electrodes at distal end of array, which were not used for stimulation.

Table S2. USEA stimulation settings. For the electrodes, u# and m# indicate an ulnar USEA electrode and median USEA electrode, respectively. For the task, "S/C" represents size/compliance identitification tasks.

Pl
Pootage closed-1, imment and h. ation due to . Video S3. First clip: Footage of HS1 performing door and handle task. Second clip: footage of first closed-loop interaction in MuJoCo. The volunteer's verbage suggests embodiment and hightened USEA-evoked perceptions compared with open-loop stimulation due to interacting with the virtual door in closed-loop.